Salinity Gradient Power: Utilizing Vapor Pressure Differences

Abstract. *By utilizing the vapor pressure difference between high-salinity and low-salinity water, one can obtain power from the gradients of salinity. This scheme eliminates the major problems associated with conversion methods in which membranes are used. The method we tested gave higher conversion efficiencies than membrane methods. Furthermore, hardware and techniques being developed for ocean thermal energy conversion may be applied to this approach to salinity gradient energy conversion.*

Energy is released when two solutions of different salt concentrations mix together. Attention has therefore been focused on salinity gradients as a source of energy. The osmotic pressure difference for freshwater rivers flowing into the sea is about 24 atm; this represents a theoretical power of more than 2 MW for a flow rate of 1 m^3/sec (*1*). The power density is even greater for rivers flowing into hypersaline lakes (*2*). Wick and Isaacs (*3*) have shown that the energy potential of the salt in salt domes is generally greater than that of the oil they might contain. Compared to other sources of energy in the ocean, excluding nuclear possibilities, salinity gradients rank with temperature gradients as having the greatest energy density and potential for conversion (*4*).

To date, virtually all of the research experiments on salinity gradient energy conversion have been based on flow-through membranes—semipermeable membranes for pressure-retarded osmosis (*5*) or ion-selective membranes for reverse electrodialysis (*6*). The difficulties associated with use of these membranes include high cost, degradation, polarization, and solution pretreatment requirements. In principle, however, most desalination schemes that are reversible are capable of producing power in salination. The scheme we report here does not require membranes. It is the reversal of vapor compression desalination, which has a higher thermodynamic efficiency than flash distillation, the most highly developed desalination method (*7*).

In vapor compression desalination, salt water is evaporated in a vacuum and the resulting vapor is compressed to raise its saturation temperature. When this freshwater vapor condenses, its latent heat of condensation is exchanged within the saltwater chamber, where it can enhance further evaporation (*7*). Vapor compression desalination has not been widely used (in spite of its relatively high thermodynamic efficiency) because of inefficient low-pressure mechanical compressors and poor heat exchangers. These limitations are now being overcome (*8*).

By applying vapor compression desalination in reverse, power can be extracted from the vapor pressure difference between water of low salinity and water of high salinity. Due to the lower vapor pressure of salt water, water vapor will rapidly transfer from fresh water to salt water in an evacuated chamber. If a turbine is interposed in the vapor flow between the two solutions, power can be extracted. A similar scheme was tried by Claude (*9*) in 1930, using vapor pressure differences resulting from the temperature gradient between ocean surface water and deep water. More recent open-cycle power plants that use ocean thermal energy have been proposed by Brown and Wechsler (*10*). Since pressure differentials and flow rates from open-cycle plants are anticipated to be low, they have proposed that the turbine blades be 24 m in diameter. Other designs have also been suggested (*11*).

Table 1. Vapor pressure (VP) differences between pure water and brine and for thermal gradients in seawater.

T^* (°C)	VP of pure water (mm-Hg)	ΔVP (mm-Hg)		
		Brine	ΔT† (°C)	Thermal gradient
			10	6
			15	10
			20	16
20	17	4		
40	55	11		
60	149	32		

*Above 80°C, seawater forms a crust from precipitation of $CaSO_4$. †ΔT compared to 4°C (VP = 6 mm-Hg) as the baseline.

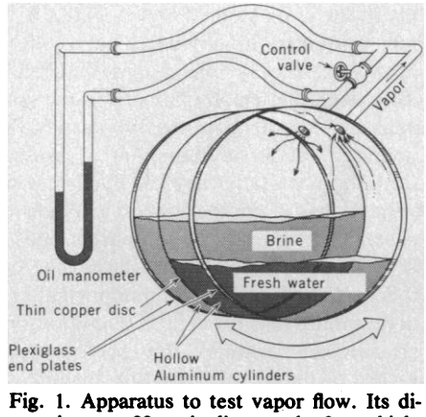

Fig. 1. Apparatus to test vapor flow. Its dimensions are 22 cm in diameter by 9 cm thick. The device was rocked through 110° at a period of about 10 seconds to wet the evaporation and condensation surface, which was made of copper for effective heat exchange. The valve controlled the flow rate (measured by change in water levels) and pressure difference (measured by an oil manometer). The entire apparatus was immersed in a water bath of constant temperature.

Vapor pressure differences between fresh water and brine (which has a salt concentration about ten times greater than seawater) are comparable to those in ocean thermal gradients (see Table 1). For the latter, a temperature difference of 20°C is considered large. Although the vapor pressure differences are similar, the usable energy density in salinity gradients is much greater. For a temperature difference of 20°C, 1 g of water transfers a net energy of 20 cal (excluding the unproductive 580 cal/g due to latent heat transfer). However, with the poor Carnot efficiency of around 20/300 (~ 6 percent), only 1.3 cal/g is useful. In contrast, 1 g of water transfers more than 9 cal of net energy between fresh water and brine (excluding latent heat) (*12*). There is no Carnot limitation on the efficiency of power derived from salinity gradients (*13*).

To test the efficacy of extracting energy by reverse vapor compression, we built a test chamber and a small model. The test chamber consisted of two short cylindrical sections connected by a thin copper heat-exchanger disk (Fig. 1); the common axis was horizontal. One compartment contained distilled water and the other contained saturated brine. In addition to exchanging heat, the two compartments communicated through a regulating valve that allowed water vapor to pass from the freshwater side to the saltwater side. The entire chamber was evacuated, held at a constant temperature, and slowly rocked to agitate the solutions and to wet the exchanger plate. We measured pressure difference with an oil manometer and volume flow by the change of liquid level on the two sides. The rate of mass transfer through the valve multiplied by the pressure differential across the valve provided the mechanical power (*14*).

Figure 2A shows the power per unit of heat exchange area as a function of the pressure difference for two temperatures. The valve setting controls the pressure difference and consequently the vapor flow. Figure 2B shows the efficiency of operation at different levels of power. The 100 percent level is normalized to 9.2 cal/g, the theoretical value for the energy density of fresh water mixing with brine. Nearly 100 percent efficiency is

0036-8075/79/1026-0452$00.50/0

possible for low rate of vapor transfer. As can be seen, a power density of as much as 7 W per square meter of heat exchanger surface was measured for some runs at 40°C. This value is much higher than values obtained with membrane systems, although theoretical calculations approach it (*12*). Weinstein and Leitz (*6*) obtained 0.2 W per square meter of membrane surface for their reverse electrodialysis model, in which seawater was used. They state that 1.7 W/m² is possible. For brine, the power density could be three times greater. Since heat-exchange materials are much cheaper and more durable than membranes, and since the process does not require extensive solution pretreatment, reverse vapor compression would probably cost less. The vapor pressure difference in reverse vapor compression increases dramatically with temperature, so it would be advantageous to place these energy units near low-grade sources of heat such as geothermal heat or waste heat from power plants.

Certain factors limit the flow rates of the reverse vapor compression. The vapor transfers heat, the latent heat of condensation, from the freshwater compartment to the saltwater compartment. Unless this heat is exchanged back, the vapor flow would diminish and eventually halt. In our experiments, most of the evaporation and condensation took place directly on the exchanger plate, and the latent heat was efficiently transferred. Another limiting factor is the outgassing of noncondensable gases that are dissolved in the water: power is needed to create and maintain the vacuum in the chamber. Chemical treatment for suspended materials and biological fouling is unnecessary since there are no membranes to clog, and fouling, if indeed it occurs in a near-vacuum, can be controlled by reversing the fresh water and the brine in the compartments.

We also built a small demonstration model that operated at an ambient temperature (27°C). It consisted of a spiral heat exchanger that doubled as a mixing pump when the unit was enclosed in a slowly rotating cylinder (Fig. 3). The vapor flowed through a small turbine that was used as a visible indicator. The turbine spun at several thousand revolutions per minute, and the power output, measured with the turbine replaced by an orifice, was 2.3 W per square meter of heat exchange surface. We measured the vapor flow rate and the pressure differential to obtain an estimate of the power. The efficiency of generation was calculated to be 23 percent.

The unique advantage of reverse vapor compression over other salinity gradient energy conversion schemes is the absence of membranes. In reverse vapor compression, the water surface itself serves as the membrane. Designs of heat exchangers and turbines are being improved for ocean thermal systems and could be easily adapted to the method discussed in this report. Our preliminary tests indicate that this scheme deserves

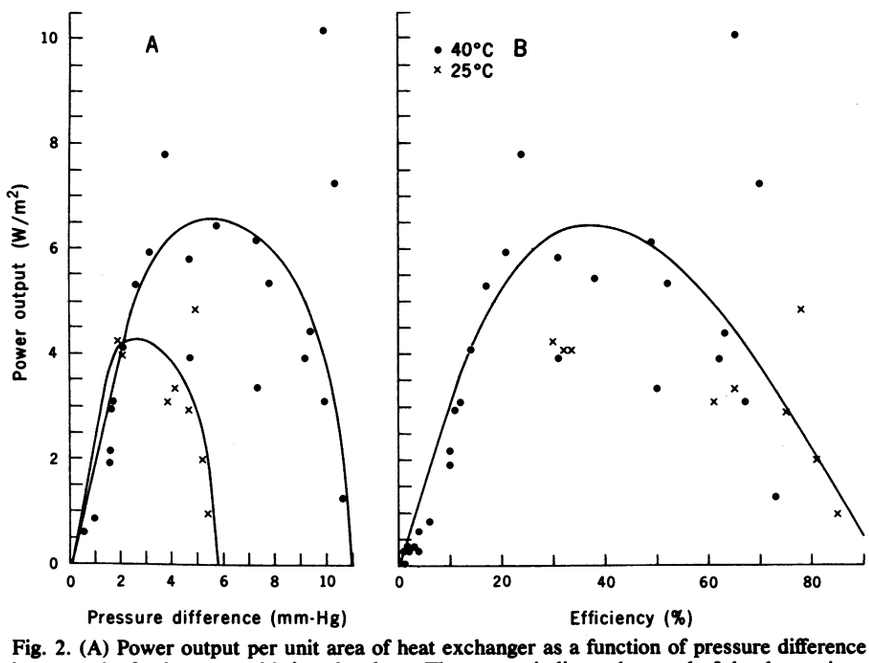

Fig. 2. (A) Power output per unit area of heat exchanger as a function of pressure difference between the freshwater and brine chambers. The curves indicate the trend of the data points. (B) The power density at different conversion efficiencies. The curve indicates the trend of the points. The scatter of the points reflects the difficulty of maintaining controlled conditions.

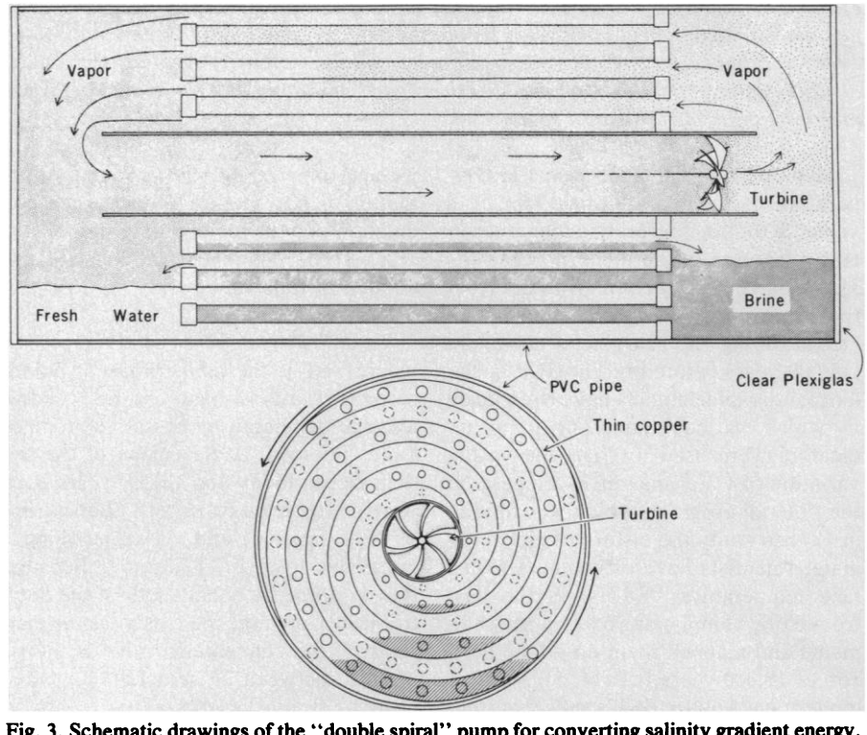

Fig. 3. Schematic drawings of the "double spiral" pump for converting salinity gradient energy. A cross section (top) and an end-on view (bottom) are shown. Rotation of the cylinder causes all the copper surfaces to be wetted by the solutions adjacent to them. Since most of the evaporation and condensation occurs on these surfaces, latent heat is efficiently transferred. The turbine is driven by vapor transferring from the freshwater side to the brine side. The model cylinder's dimensions are 20 cm in diameter by 40 cm in length. Pipe is polyvinyl chloride (*PVC*).

more attention as a possible energy source that could have a significant impact in areas such as the U.S. Gulf Coast, where brine and fresh water or seawater exist in abundance.

MARK OLSSON
Institute of Marine Resources, Scripps Institution of Oceanography, University of California, San Diego, La Jolla 92093, and *Foundation for Ocean Research, San Diego 92121*
GERALD L. WICK
Institute for Transcultural Studies, Los Angeles, California 90006
JOHN D. ISAACS
Institute of Marine Resources, Scripps Institution of Oceanography, and *Foundation for Ocean Research*

References and Notes

1. G. L. Wick and J. D. Isaacs, *Utilization of Energy from Salinity Gradients* (IMR 76-9, Institute of Marine Resources, University of California, La Jolla, 1976).
2. S. Loeb, *Science* **189**, 654 (1975).
3. G. L. Wick and J. D. Isaacs, *ibid.* **199**, 1436 (1978); *ibid.* **203**, 376 (1979).
4. G. L. Wick and W. R. Schmitt, *Mar. Technol. Soc. J.* **11**, 16 (1977).
5. S. Loeb, *J. Membr. Sci.* **1**, 49 (1976); Inter-Technology/Solar Corporation, *Solar Electricity: Osmo-hydro Power from Aqueous Saline Solutions, Assessment of Its Potential* (Report 289378, Department of Energy, Washington, D.C., 1978).
6. J. Weinstein and F. Leitz, *Science* **191**, 557 (1976).
7. B. W. Tleimat, paper presented at the American Society of Mechanical Engineers Winter Annual Meeting, Los Angeles, 16–20 November 1969.
8. A. Laird, personal communication.
9. G. Claude, *Mech. Eng.* **52**, 1039 (1930).
10. C. E. Brown and L. Wechsler, in *Proceedings of the Seventh Annual Offshore Technology Conference* (1975), vol. 2, p. 111.
11. *Proceedings of the Fifth Ocean Thermal Energy Conversion Conference* (Conf. 780236, Department of Energy, Washington, D.C., 1978).
12. G. L. Wick, *Energy Int. J.* **3**, 95 (1978).
13. Carnot efficiency applies to the latent heat transferred back to the evaporation chamber.
14. This estimate of power was conservative, since the useful energy was not extracted by a turbine in these experiments. This energy thus appeared as heat on the saltwater side and tended to oppose the vapor transfer.
15. We thank the trustees of the Foundation for Ocean Research for their support, S. Sinell for assisting in the experiments, and R. Ando for valuable discussions. This research was partially supported by grant 04-6-158-4410 (project R/E-6) from the Office of Sea Grant, National Oceanic and Atmospheric Administration.

27 March 1979; revised 4 June 1979

Zonal Temperature-Anomaly Maps of Indian Ocean Surface Waters: Modern and Ice-Age Patterns

Abstract. *Maps of sea surface temperature anomalies in the Indian Ocean in modern and ice-age times reveal striking changes in its surface circulation. During the last glacial maximum (18,000 years before the present), the Indian Ocean had colder average zonal surface temperatures, a cooler and less extensive Agulhas Current, a distinct eastern boundary current, and decreased upwelling and a weaker southwest monsoon in its northwestern region.*

Maps of zonal anomalies in the temperature of the sea's surface can be a valuable tool in interpreting major circulation features in the modern ocean (*1–3*). We have used such maps to interpret the surface circulation of the Indian Ocean during the last glacial maximum [18,000 years before present (B.P.)]. Paleoceanographic studies have been made in which various faunal or floral indicators were used to chart the spatial variation of water masses in the past. In the CLIMAP program, which was formed in 1971 to study the history of global climate, scientists have estimated sea surface temperatures (SST's) in the past from biotic components of deep-sea sediments and mapped them on a time horizon of 18,000 years B.P. (*4, 5*). Maps of modern and ice-age SST's reflect current systems and water masses; maps of the temperature differences between them can be useful in interpreting the oceanic response to climatic change (*4*). In this report we compare zonal SST anomaly maps of the Indian Ocean in modern and ice-age times to obtain additional information on how ice-age surface water circulation may have been different.

Zonal SST anomalies (ΔSST_z) are calculated as follows:

$$\Delta SST_z = (SST - \overline{SST}_z)$$

where SST is the temperature at points along a latitudinal band and $\overline{SST}_z$ is the average temperature of the latitudinal band. Seasonal ΔSST_z maps of the Indian Ocean today and 18,000 years B.P. were constructed by using a grid spacing of 2° of longitude and averaging along a zonal width of 2° of latitude. Because flow is primarily zonal south of the Subtropical Convergence, only anomalies north of the convergence (that is, north of 50°S, between 20° and 120°E) are reported.

The data we used to construct ΔSST_z represent sea surface conditions for the Indian Ocean in both times. Data for present-day February and August SST's are shown in Fig. 1, A and B (*6*). Isotherms for the last glacial maximum (Fig. 1, C and D) are based on 42 SST estimates from planktonic foraminiferal transfer function FI-2 (*7*), faunal province boundaries, and analogies to modern SST gradients. The standard error of individual estimates for FI-2 is ± 1.1°C for February and ± 1.3°C for August. However, adjacent cores in low-gradient areas normally differ by $<\pm$ 0.5°C. Accordingly, although we feel that the distribution of data points (Fig. 1) and the smoothness of gradients precludes major errors, we have not placed great emphasis on interpreting ΔSST_z of < 1°C. South of the Subtropical Convergence, additional data based on radiolaria (*8*) support the gradients determined from the estimates based on foraminifera. The February and August ΔSST_z maps for modern and ice-age times are shown in Fig. 2.

Maps of ΔSST_z reveal temperature contrast along a zonal band and identify areas that are colder or warmer than the latitudinal average. If there were no large ocean currents and continental boundaries, ocean surface temperatures would reflect the pattern of solar radiation and show meridional temperature gradients. Isotherms would be zonal and all temperatures along a latitudinal zone would be equal; ΔSST_z would be zero. In the real ocean, however, current systems and continental boundaries preclude so simple a zonal pattern. Anomalies are created by advection of warm or cold waters into a latitudinal zone. In general, horizontal advection transports warm waters poleward, producing positive anomalies (for example, the Gulf Stream) along western boundaries, and transports cold waters equatorward, producing negative anomalies (for example, the Peru Current) along eastern boundaries. In addition, vertical advection brings cold water to the surface, creating negative anomalies along some continental margins. Thus, a map of ΔSST_z should reflect these circulation features.

The maps of ΔSST_z in the Indian Ocean for February and August in modern times (Fig. 2, A and B) reveal the major circulation features north of the Subtropical Convergence. Examination of Fig. 2A reveals that in February (i) a large positive ΔSST_z southeast of Africa coincides with the southerly flowing Agulhas Current; (ii) in the eastern section of the subtropical gyre, equatorward flow (indicated by negative ΔSST_z's) is centered at approximately 105°E; (iii) across the central Indian Ocean, negative anomalies trend from southeast to northwest and generally coincide with the South Equatorial Current; and (iv) north of the equator, the northwestern Indian Ocean

0036-8075/79/1026-0454$00.50/0